Proceedings of the 17th World Congress
The International Federation of Automatic Control
Seoul, Korea, July 6-11, 2008

Integrated Active Front Steering and Semiactive Rear Differential Control in Rear Wheel Drive Vehicles

R. Marino * **S. Scalzi** **

* *University of Rome Tor Vergata, Electronic Engineering Department - DIE, Via del Politecnico 1, 00133 Roma - Italy, Tel. 0039 06 7259 7412 (e-mail: marino@ing.uniroma2.it)*
** *University of Rome Tor Vergata, Electronic Engineering Department - DIE, Via del Politecnico 1, 00133 Roma - Italy (e-mail: scalzi@ing.uniroma2.it).*

Abstract: Many vehicle control systems are based on the yaw rate error to help the driver during oversteer and understeer conditions. The control systems usually operate on brake pressures distributions such as ESP and/or on active front and rear steering control. Recently many papers are focused on the design of integrated global chassis control systems. The main contribution of this paper is to show for a CarSim® small SUV model the stability of a proportional-integral active front steering control from the yaw rate tracking error integrated with an electronically controlled semiactive rear differential from the rear wheel speed measurements; the stability analysis is based on Lyapunov techniques. The integrated controlled system shows increased performances: new stable cornering manoeuvres and increased safety especially in emergency conditions. Several simulations are carried out on a standard CarSim® small SUV model to confirm the analysis and to explore the robustness with respect to unmodelled combined lateral and longitudinal tire forces according to combined slip theory and unmodelled dynamics such pitch and roll. The simulations on CarSim® vehicle show the benefits of using the proposed integrated control with respect to the case in which only active front steering is employed.

Keywords: Vehicle Dynamics; Integrated Automotive Control; Front Steering; Semiactive Rear Differential.

1. INTRODUCTION

Many vehicle control systems were designed and implemented in the last years to enhance performances, stability, controllability, handling, comfort and safety. Several front steering control laws are proposed as in Ackermann (1990), Baumgarten (2004), Pauly et al. (2005) and implemented on vehicles or on steer by wire prototypes. In Ackermann (1990) it is shown that the lateral acceleration of the front axle may be robustly triangularly decoupled from the yaw rate dynamics, using only the front wheel steering angle as a control input, by feeding back the yaw rate error through an integrator. In Baumgarten (2004) a PI active steering control on the yaw rate tracking error with different gains for braked and unbraked driving condition is used. In Pauly et al. (2005) the active front steering is designed in order to ensure safety also during a system failures: in fact, the wheel steering angle δ_f is the sum of the designed feedback control δ_c and the driver input δ_p.
The development of electro actuated differentials allows for new control strategies as in Frediani et al. (2002), Ushiroda et al. (2003), Cheli et al. (2005), Milanese et al. (2006), Marino et al. (2007) in vehicle systems dynamics control. In Cheli et al. (2005) the differential control system is semiactive since the electronic control system can decide the locking torque transferred but not its direction; the transfered torque is generated from the fastest wheel to the slowest one; the control operates when the rear wheels speed difference exceeds a given threshold and its value is computed by a proportional-integral control law on the measured and the desired rear wheel speed angular velocity. In Milanese et al. (2006), the proposed controller is designed following the Internal Model Control approach and it is active since it can generate yaw moments of every amount and direction. In Marino et al. (2007) the locking action of the rear differential is electronically controlled according to a Lyapunov analysis.
Many papers are currently focused on the design of integrated global chassis control systems: in Nagai et al. (2002) an integrated control of active front steering and direct yaw moment generated by a distribution of braking forces is designed; in Jingxin Shi (2006) the electronic stability program (ESP) is integrated with the active front wheel steering, the active suspension and an active anti roll bar; in Daofei Li et al. (2006) four wheel steering is coordinated with wheel torque distribution using an optimization approach; a non linear optimization approach is followed by Hattori Yoshikazu et al. (2003) to determine the optimal force to be exerted by each tire controlled by active steering and brake pressures distribution.
While the advantages of active front steering control and electronically controlled differential (either active or semiactive) are well established, the stability of their integrated action is yet to be investigated. This is the aim of this paper in which we design and integrate an active front steering control system and a semiactive electronically controlled rear differential on the basis of a Lyapunov stability analysis.
The paper is organized as follows: the non linear full car model is introduced and the linear approximation is computed; a re-

duced model is obtained by decoupling the longitudinal and lateral dynamics; then the proportional-integral active front steering control on the yaw rate error and the proportional semiactive rear differential control on the error between the measured and the desired rear wheel angular speed difference are designed and the stability of the controlled system is ensured by a Lyapunov stability analysis; finally some simulations on typical manoeuvres are presented for a standard CarSim® small SUV to confirm the analysis, to explore the robustness with respect to unmodelled dynamics and to show the improvements due to the use of the proposed integrated control system with respect to a vehicle equipped with only an active front steering control. The interactions with a simple driver model are also analyzed by a standard Moose test.

2. NONLINEAR AND LINEAR CAR MODELS

A detailed non linear full car model (Fig. 1) with nonlinear tire characteristics, combined slip and differential load transfer for each wheels are considered. To capture the essential vehicle steering dynamics and to design the controller a simplified non linear seven degree of freedom model is presented and analyzed in this section. The non linear model is described by the following equations:

$$\begin{cases} \dot{v}_x &= rv_y + (F_{xfl}\cos\delta_f + F_{xfr}\cos\delta_f + F_{yfl}\sin\delta_f + \\ & +F_{yfr}\sin\delta_f + F_{xrl} + F_{xrr} - c_a {v_x}^2)/m \\ \dot{v}_y &= -rv_x + (F_{xfl}\sin\delta_f + F_{xfr}\sin\delta_f - F_{yfl}\cos\delta_f - \\ & -F_{yfr}\cos\delta_f - F_{yrl} - F_{yrr})/m \\ \dot{r} &= (l_f(F_{xfl}\sin\delta_f + F_{xfr}\sin\delta_f - F_{yfl}\cos\delta_f - \\ & -F_{yfr}\cos\delta_f) + l_r(F_{yrl} + F_{yrr}) - (F_{xfl}\cos\delta_f - \\ & -F_{xfr}\cos\delta_f + F_{yfl}\sin\delta_f - F_{yfr}\sin\delta_f)T_f/2 - \\ & (F_{xrl} - F_{xrr})T_r/2)/J \\ \dot{\omega}_{fl} &= -(R_w F_{xfl})/J_w \\ \dot{\omega}_{fr} &= -(R_w F_{xfr})/J_w \\ \dot{\omega}_{rl} &= -(R_w F_{xrl} - T_{eng}/2 - T_{diff})/J_w \\ \dot{\omega}_{rr} &= -(R_w F_{xrr} - T_{eng}/2 + T_{diff})/J_w \end{cases} \tag{1}$$

$$F_{yi}(\alpha_i) = D_y \sin\{C_y \text{atan}[(1-E_y)B_y\alpha_i + E_y \text{atan}(B_y\alpha_i)]\} \tag{2}$$

$$F_{xi}(\lambda_i) = D_x \sin\{C_x \text{atan}[(1-E_x)B_x\lambda_i + E_x \text{atan}(B_x\lambda_i)]\} \tag{3}$$

$$\begin{cases} \lambda_i = (\omega_i R_w - V_i)/V_i \\ V_i = \left(\left(v_y \pm r l_f\right)^2 + \left(v_x \pm r T_f/2\right)^2\right)^{1/2} \end{cases} \tag{4}$$

$$\begin{cases} \beta_{fl} &= \left(\left(v_y + r l_f\right)/\left(v_x - r T_f/2\right)\right) \\ \beta_{fr} &= \left(\left(v_y + r l_f\right)/\left(v_x + r T_f/2\right)\right) \\ \beta_{rl} &= \left(\left(v_y - r l_r\right)/\left(v_x - r T_r/2\right)\right) \\ \beta_{rr} &= \left(\left(v_y - r l_r\right)/\left(v_x + r T_r/2\right)\right) \end{cases} \tag{5}$$

$$\begin{cases} \alpha_{fl} = \beta_{fl} - \delta_f; & \alpha_{rl} = \beta_{rl}; \\ \alpha_{fr} = \beta_{fr} - \delta_f; & \alpha_{rr} = \beta_{rr} \end{cases} \tag{6}$$

where: v_y (v_x) are the lateral (longitudinal) vehicle velocity, v is the vehicle velocity, r is the vehicle yaw rate, β is the vehicle slip angle, δ_f is the front steer angle, F_y (F_x) are the lateral (longitudinal) forces given by Pacejka tire model (2) and (3), Pacejka (2004), α_f (α_r) is the front (rear) wheel sideslip angle, λ_f (λ_r) is the longitudinal front (rear) wheel slip angle, V_i are the wheels velocities, l_f (l_r) is the longitudinal distance from the front (rear) axle to the center of mass, T_f (T_r) is the front (rear) distance from the wheels on the same axle, c_a is the aerodynamics drag coefficient, m is vehicle mass, J is the vehicle inertia with respect to the vertical axle through to the center of mass, J_w are the wheels inertia, R_w are the wheels radius, a_y is the lateral acceleration, T_{eng} is the net torque due to the engine to the rear axle shafts and T_{diff} is the transferred torque between the rear wheels.

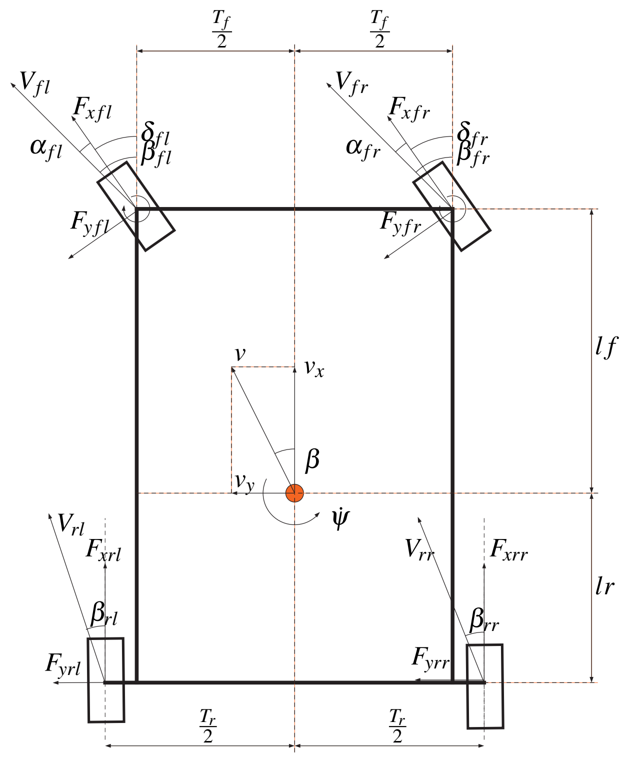

Fig. 1. Full car model.

If the system (1) is linearized around uniform rectilinear motion; the linearized system, $\dot{x} = Ax + Bu$, is given by:

$$A = \begin{bmatrix} a_{11} & 0 & 0 & a_{14} & a_{15} & a_{16} & a_{17} \\ 0 & a_{22} & a_{23} & 0 & 0 & 0 & 0 \\ 0 & a_{32} & a_{33} & a_{34} & a_{35} & a_{36} & a_{37} \\ a_{41} & 0 & a_{43} & a_{44} & 0 & 0 & 0 \\ a_{51} & 0 & a_{53} & 0 & a_{55} & 0 & 0 \\ a_{61} & 0 & a_{63} & 0 & 0 & a_{66} & 0 \\ a_{71} & 0 & a_{73} & 0 & 0 & 0 & a_{77} \end{bmatrix}, \tag{7}$$

$$x = \begin{bmatrix} v_x \\ v_y \\ r \\ \omega_{fl} \\ \omega_{fr} \\ \omega_{rl} \\ \omega_{rr} \end{bmatrix}, \quad B = \begin{bmatrix} 0 & 0 \\ b_{21} & 0 \\ b_{31} & 0 \\ 0 & 0 \\ 0 & 0 \\ 0 & b_{62} \\ 0 & b_{72} \end{bmatrix}, \quad u = \begin{bmatrix} \delta_f \\ T_{diff} \end{bmatrix}. \tag{8}$$

By changing the coordinates $\bar{x} = Tx$, we obtain the following linear system, $\dot{\bar{x}} = \bar{A}\bar{x} + \bar{B}u$, in which the new state space variable are the sum and the difference between the front and rear wheel speed:

$$\bar{x} = Tx = \begin{bmatrix} (\omega_{fl}+\omega_{fr})/2 \\ (\omega_{rl}+\omega_{rr})/2 \\ v_x \\ v_y \\ r \\ \omega_{fl}-\omega_{fr} \\ \omega_{rl}-\omega_{rr} \end{bmatrix} = \begin{bmatrix} \bar{\omega}_f \\ \bar{\omega}_r \\ v_x \\ \bar{x}_1 \\ \bar{x}_2 \\ \bar{x}_3 \\ \bar{x}_4 \end{bmatrix}$$

$$\frac{d\bar{x}}{dt} = \begin{bmatrix} \bar{a}_{11} & 0 & \bar{a}_{13} & 0 & 0 & 0 & 0 \\ 0 & \bar{a}_{22} & \bar{a}_{23} & 0 & 0 & 0 & 0 \\ \bar{a}_{31} & \bar{a}_{32} & \bar{a}_{33} & 0 & 0 & 0 & 0 \\ 0 & 0 & 0 & \bar{a}_{44} & \bar{a}_{45} & 0 & 0 \\ 0 & 0 & 0 & \bar{a}_{54} & \bar{a}_{55} & \bar{a}_{56} & \bar{a}_{57} \\ 0 & 0 & 0 & 0 & \bar{a}_{65} & \bar{a}_{66} & 0 \\ 0 & 0 & 0 & 0 & \bar{a}_{75} & 0 & \bar{a}_{77} \end{bmatrix} \bar{x} + \begin{bmatrix} 0 & 0 \\ 0 & 0 \\ 0 & 0 \\ \bar{b}_{41} & 0 \\ \bar{b}_{51} & 0 \\ 0 & 0 \\ 0 & \bar{b}_{72} \end{bmatrix} \begin{bmatrix} \delta_f \\ T_{diff} \end{bmatrix}. \quad (9)$$

The system (9) is decoupled in two subsystems: the first one is an autonomous system and describes the longitudinal dynamics, and the second one represents the lateral dynamics.

3. CONTROL DESIGN

3.1 Active Front Steering Control Design

The active front steering is designed in order to ensure safety also during a system failure; in fact the wheel steering angle δ_f is the sum of the designed feedback control δ_c and the driver input δ_p as in Pauly et al. (2005). The proposed PI feedback control algorithm can be written as follows:

$$\begin{cases} \delta_c = -K_{pf}\tilde{r} - K_{if}\alpha_0 \\ \dot{\alpha}_0 = \tilde{r} \end{cases} \quad (10)$$

where: $\delta_f = \delta_p + \delta_c$, $\tilde{r} = r - r_d$ and r_d is equal to the uncontrolled vehicle yaw rate equilibrium point value and can be written such as $r_d = G\delta_p$ in which G is the static gain of the transfer function between δ_p and r. To take into account the nonlinearity for the nonlinear vehicle model a nonlinear reference model will be employed. The controlled system (9,10) $\dot{\bar{x}}_c = \bar{A}_c\bar{x}_c + \bar{B}_c u_c$ is the following:

$$\frac{d\bar{x}_c}{dt} = \begin{bmatrix} \bar{a}_{c11} & \bar{a}_{c12} & 0 & 0 & \bar{a}_{c15} \\ \bar{a}_{c21} & \bar{a}_{c22} & \bar{a}_{c23} & \bar{a}_{c24} & \bar{a}_{c25} \\ 0 & \bar{a}_{c32} & \bar{a}_{c33} & 0 & 0 \\ 0 & \bar{a}_{c42} & 0 & \bar{a}_{c44} & 0 \\ 0 & 1 & 0 & 0 & 0 \end{bmatrix} \bar{x}_c + \begin{bmatrix} \bar{b}_{c11} & 0 \\ \bar{b}_{c21} & 0 \\ 0 & 0 \\ 0 & \bar{b}_{c42} \\ -G & 0 \end{bmatrix} u_c \quad (11)$$

where $\bar{x}_c$ and u_c are defined by:

$$\bar{x}_c = \begin{bmatrix} v_y \\ r \\ \bar{x}_3 \\ \bar{x}_4 \\ \alpha_0 \end{bmatrix}, \quad u_c = \begin{bmatrix} \delta_p \\ T_{diff} \end{bmatrix}. \quad (12)$$

3.2 Semiactive Differential Control Design

From the non linear car model (1) the rear wheels angular speed dynamics are described as follows:

$$\begin{aligned} J_w\dot{\omega}_{rl} &= -R_wF_{xrl} + T_{eng}/2 + T_{diff} \\ J_w\dot{\omega}_{rr} &= -R_wF_{xrr} + T_{eng}/2 - T_{diff}\,. \end{aligned} \quad (13)$$

The actuator's power P_{act} is equal to:

$$P_{act} = T_{diff}\bar{x}_4 \quad (14)$$

and the torque T_{diff} is transferred only when (14) is negative due to the passivity of the actuator. The torque T_{diff} is transferred from the fastest wheel to the slowest ones in fact if $\bar{x}_4 > 0$ (i.e. $\omega_{rl} > \omega_{rr}$) and T_{diff} is negative the control law is active and the torque is transferred from ω_{rl} to ω_{rr} as we may observe from (13).

The semiactive rear differential control algorithm (see Cheli et al. (2005)) is defined as:

$$T_{diff} = \begin{cases} T^*_{diff} & if \quad T^*_{diff}\bar{x}_4 \le 0 \\ 0 & if \quad T^*_{diff}\bar{x}_4 > 0\,. \end{cases} \quad (15)$$

with:

$$T^*_{diff} = -K_{pd}\bar{x}_4 \quad (16)$$

3.3 Stability Analysis

The stability of the proposed discontinuous control law is based on the time derivative of the following quadratic function V:

$$V = \tilde{x}^T P \tilde{x}$$

in which P is a positive definite symmetric matrix, $\tilde{x} = \bar{x}_c - \bar{x}_d$ are the error variables, $\bar{x}_d = -\bar{A}_c^{-1}\bar{b}_{c1}\delta_p$ are the reference signals and $\bar{b}_{ci}$ are the column vectors i-th of the matrix $\bar{B}_c$. The time derivative of V is computed as follows:

$$\begin{aligned} \dot{V} = \tilde{x}^T P \left(\bar{A}_c\tilde{x} + \bar{A}_c\bar{x}_d + \bar{B}_c u_c\right) + \\ + \left(\tilde{x}^T\bar{A}_c^T + \bar{x}_d^T\bar{A}_c^T + u_c^T\bar{B}_c^T\right)P\tilde{x} \end{aligned}$$

$$\begin{aligned} \dot{V} = \tilde{x}^T P \left(\bar{A}_c\tilde{x} + \bar{A}_c(-\bar{A}_c^{-1}\bar{b}_{c1}\delta_p) + \bar{b}_{c1}\delta_p + \bar{b}_{c2}T_{diff}\right) + \\ + \left(\tilde{x}^T\bar{A}_c^T + (-\bar{A}_c^{-1}\bar{b}_{c1}\delta_p)^T\bar{A}_c^T + \bar{b}_{c1}\delta_p + \bar{b}_{c2}T_{diff}\right)P\tilde{x} \end{aligned}$$

$$\dot{V} = \tilde{x}^T\left(P\bar{A}_c + \bar{A}_c^T P\right)\tilde{x} + 2\tilde{x}^T P\bar{b}_{c2}T_{diff}\,. \quad (17)$$

In Fig. 2 we may observe that the transfer function between T_{diff} and $\bar{x}_4$, for the nominal vehicle parameters shown in Appendix (Table 1) of a small SUV model given by Carsim®, is SPR (Strictly Real Positive): in fact, for every speed of interest, the Nyquist diagrams belong to the right half plane for every frequency.

Then, for any symmetric positive define n x n matrix Q there exist an n x n symmetric positive definite matrix P, an n x 1 real vector q and a positive real ε, Marino et al. (1995), such that:

$$\begin{aligned} \bar{A}^T P + P\bar{A} &= -qq^T - \varepsilon Q = -Q^* \\ Pb &= c^T\,. \end{aligned} \quad (18)$$

The equation (17) can be rewritten as follows:

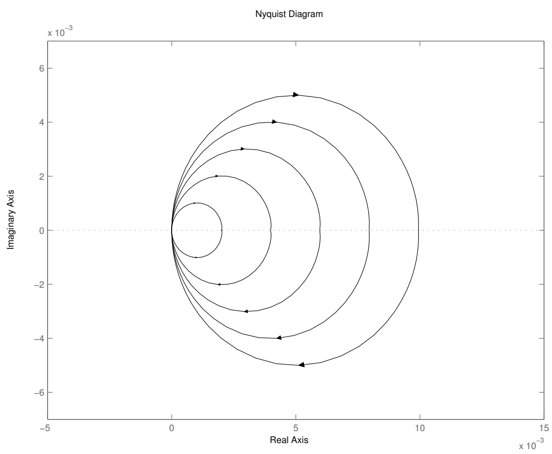

Fig. 2. Nyquist diagrams for different velocities ($5 < v < 50$ $[m/s]$).

$$\dot{V} = -\tilde{x}^T Q^* \tilde{x} + 2T_{diff} c\tilde{x} \,. \qquad (19)$$

Defining:

$$c = [0 \quad 0 \quad 0 \quad 1] \,, \qquad (20)$$

equation (19) can be rewritten as follows:

$$\dot{V} = -\tilde{x}^T Q^* \tilde{x} + 2\tilde{x}_4 T_{diff} = -\tilde{x}^T Q^* \tilde{x} - 2K_{pd}\tilde{x}_4^2 \,. \qquad (21)$$

When the control law (15) is on, the speed of convergence of the controlled vehicle is greater than the uncontrolled one while, if the control law (15) is off the speed of convergence is equal to the uncontrolled one in fact, form (21) we may observe the following relations:

$$V(\phi(t, x_0))_{OFF} \geq V(\phi(t, x_0))_{ON} \,.$$

4. SIMULATION RESULTS

4.1 Nonlinear Reference Model

To take the nonlinearities into account a non linear first order reference model is used to compute the needed reference signals: in fact the driver input signal δ_p drives a non linear first order reference model which, according to the velocity v and the tire-road adherence conditions, generates the yaw rate reference signal r_d and the desired difference angular velocity $\bar{x}_{4d}$. The reference model is defined as:

$$\dot{\bar{x}}_{id} = -a_{ref}(v)\left(\bar{x}_{id} - G_i(\delta_p, v)\,\delta_p\right) \qquad i = 2, 4 \,. \qquad (22)$$

Where a_{ref} is a design parameter for the non linear reference model and $G_i(\delta_p, v)$ can be computed storing, directly from uncontrolled vehicle measurements (e.g. using steering pad tests), the desired yaw rate and wheel speed references, as shown in Fig. 3, in a look up table.

The functional scheme for the proposed controlled system is described in Fig. 4. For the simulations two thresholds are defined: the maximum allowed rear angular wheel speed difference and the minimum yaw rate error; if $\bar{x}_4$ is greater than the threshold a locking action is done to improve traction while if r is smaller than the threshold the control law is off; the thresholds depend on v and δ_p.

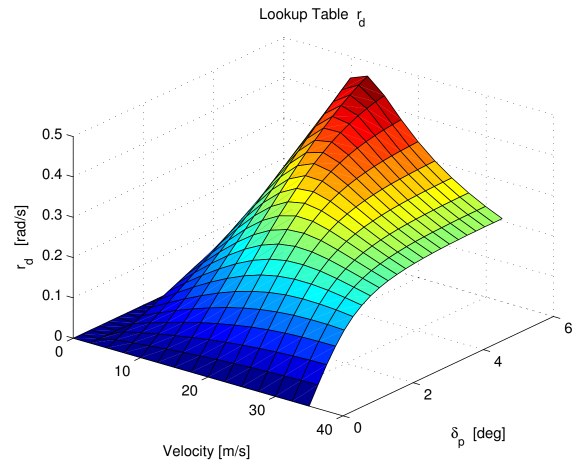

Fig. 3. Yaw rate references for different steering angles and velocities on dry road.

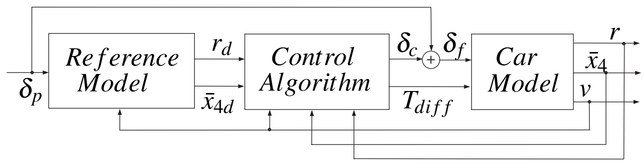

Fig. 4. Functional scheme for the designed control system.

4.2 Simulation Results on Carsim® Vehicle

A full vehicle model of a standard Carsim® small SUV model is used to analyze the responses of both the uncontrolled and the controlled vehicle and to check robustness with respect to combined lateral and longitudinal tire forces effects and to unmodelled dynamics such as pitch and roll. CarSim® vehicle takes into account the major kinematics and compliance effects of the suspensions (nonlinear spring models) and steering systems and uses nonlinear combined lateral and longitudinal tire model according to combined slip theory.

The simulations are performed using in (22) the uncontrolled vehicle static gain $G_i(\delta_p, v)$ obtained by storing the steady state yaw rate and rear wheel angular velocity difference values in a lookup table for different steering angles and car velocities. Many canonical manoeuvres, such as sudden direction change, overtaking and μ split, are performed to check the robustness of the proposed control system and to analyze the effect of the semiactive differential on the vehicle behavior.

The controlled system shows many advantages if the integrated control system is employed: new stable cornering manoeuvres and improved performance. Even thought the simulated vehicle model shows an understeering response to increasing steer angles, on wet road, $\mu = 0.7$, it is shown, in Fig. 5 and Fig. 6, a new stable cornering manoeuvre for the controlled vehicle. In Fig. 5 we may observe the driver steering wheel angle and the correction provided by the active front steering while in Fig. 6 it is shown the action of the semiactive rear differential.

In a μ split manoeuvre one side vehicle wheels are on a low adherence surface such as ice or mud; in a power on driving condition a free differential can not transmit the driving torque to the wheel with high adherence and the vehicle does not move; the locking action may generate an undesired over-

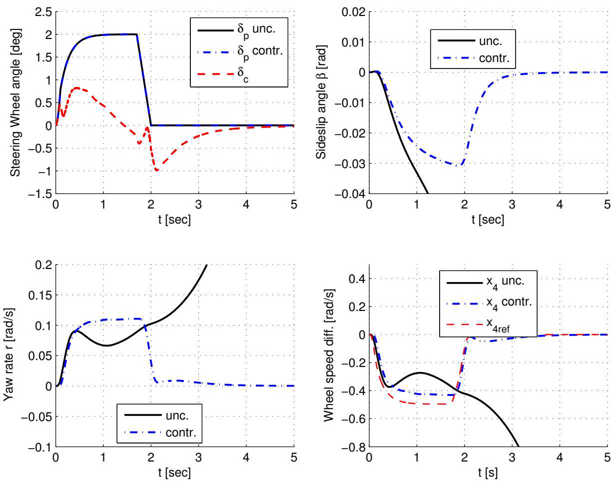

Fig. 5. Sudden direction change: uncontrolled and controlled Carsim® car model on wet asphalt at $v = 30$ $[m/s]$.

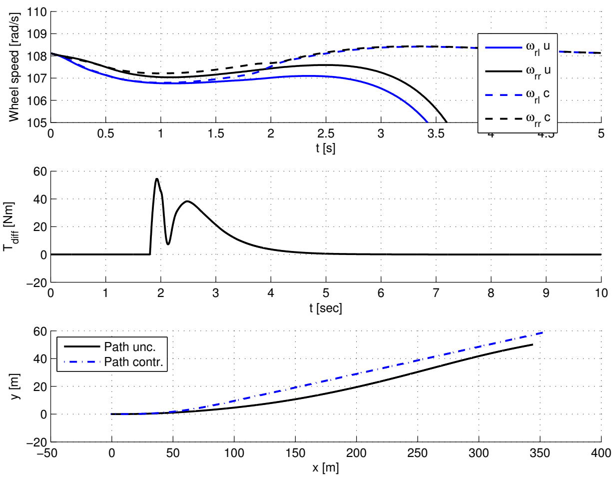

Fig. 6. Sudden direction change: uncontrolled and controlled Carsim® car model on wet asphalt at $v = 30$ $[m/s]$.

steering torque when a mechanical differential is used while, by an electronically controlled differential, the activation can be properly designed. In Fig. 7 and Fig. 8 a μ split braking manoeuvre is analyzed. The simulation is performed setting the high friction coefficient $\mu = 1$ on the right hand side and the low friction coefficient $\mu = 0.2$ on the left hand side; a sudden braking action is analyzed on the uncontrolled (unc.) vehicle, the controlled vehicle with the integrated control (integr.) and on a vehicle with the active front steering (AFS) only. Both the controlled vehicles keep the track while the uncontrolled vehicle goes out of track as shown in Fig. 8. If the proposed integrated control is employed the active steering action is reduced and, especially for increasing emergency braking action, the errors from the desired state variables, are greatly reduced with respect to a vehicle equipped with only the active front steering showing improvements with respect the use of a single control system. The integrated controlled systems shows a better performance on the XY plane (Fig. 8).

The moose test is also performed to check the robustness of the proposed control law with respect to a driver controller modelled in CarSim. CarSim uses an optimal control to follow

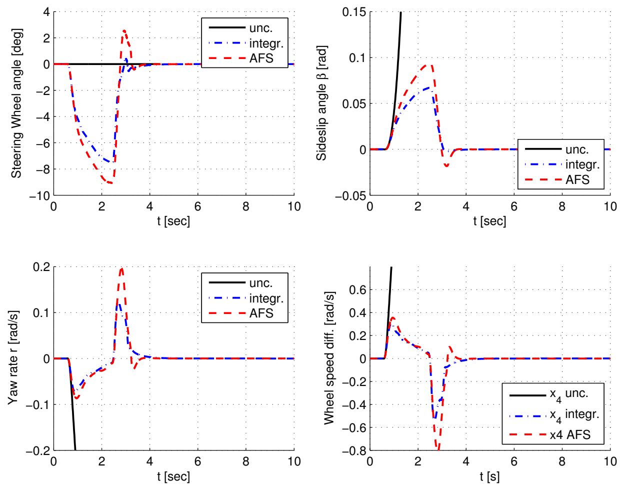

Fig. 7. μ split on: uncontrolled (u), integrated controlled (integr.) and active front steering (AFS) controlled Carsim® car model at $v = 30$ $[m/s]$.

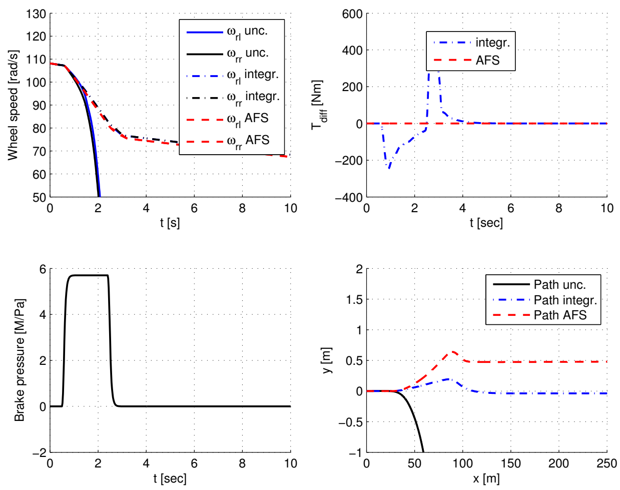

Fig. 8. μ split on: uncontrolled (u), integrated controlled (integr.) and active front steering (AFS) controlled Carsim® car model at $v = 30$ $[m/s]$.

a prescribed path; in this case the path is part of the ISO/DIS 3888 standard. The test is a XY plane path with pre-determined cone placement on a dry road. The controlled vehicle can reach higher longitudinal speed without fail the test (hit the obstacles or/and rollover). The result for $v = 30$ $[m/s]$ are shown in Fig. 9 and Fig. 10: the uncontrolled vehicle rolls over while the controlled one passes the test.

5. CONCLUSIONS

An integration between an active front steering system and an electronically controlled rear semiactive differential is designed on the basis of Lyapunov analysis. The controller feeds back the yaw rate, the wheel angular velocity and the vehicle velocity; the needed reference signals are generated on the basis of a first order nonlinear reference model driven by the driver steering wheel input.
If the proposed integrated control is employed, especially for emergency manoeuvres, the errors from the desired state variables, are greatly reduced with respect to a vehicle equipped with only the active front steering showing improvements with

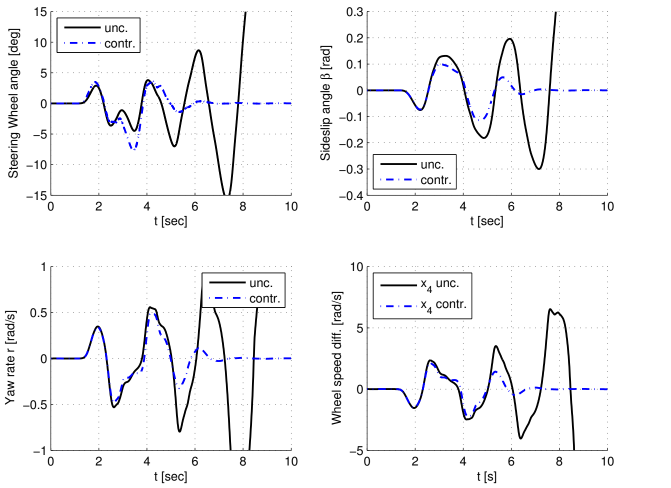

Fig. 9. Moose test for the uncontrolled and controlled Carsim® car model $v = 30$ $[m/s]$.

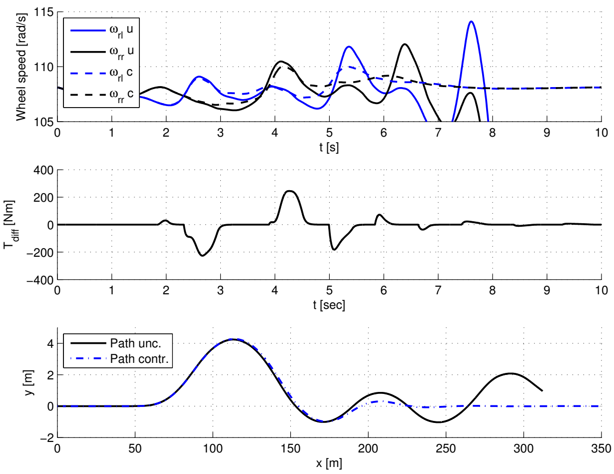

Fig. 10. Moose test for the uncontrolled and controlled Carsim® car model $v = 30$ $[m/s]$.

respect the use of a single control system.

A drawback for the proposed control system, which is common to the most automotive control systems, is the dependence of the reference model from the coefficient of adherence: to overcame it on line estimation schemes should be incorporated in the controller.

REFERENCES

G. Baumgarten, "Motor vehicle steering system having a yaw rate controller", Bayerische Motoren Werke, United States Patent Pub. No. US 20040070268 April 15/2004

A. Pauly, G. Baumgarten, "Overlay steering system and method for motor vehicles", Bayerische Motoren Werke Aktiengesellschaft, United States Patent Pub. No. US 6854558 Feb 15/2005

J. Ackermann, "Robust Car Steering by yaw rate control", IEEE Conference on Decision and Control, pp. 2033-2034, 1990

Shi Jingxin, "Integrated Global Chassis Control - A Top-Down Design Approach" Proceeding of FISITA World Automotive Congress, Yokohama, Japan, 22-27 October 2006

Yoshikazu Hattori, "Optimum Vehicle Dynamics Control Based on Tire Driving and Braking Forces" Toyota CRDL, Vol. 38, No. 4

Daofei Li, Xiaoming Shen and Fan Yu, "Study on the Chassis Control Integration Based on Tire Slip Ratio Regulation and Active Steering Control" Proceeding of FISITA World Automotive Congress, Yokohama, Japan, 22-27 October 2006

Hans B. Pacejka, "Tyre and Vehicle Dynamics", Elsevier - Butterworth Heinemann, 2004

R. Marino, P.Tomei, "Non Linear Control Design, Geometric, Adaptive, Robust", London, UK, Prentice Hall, pp. 362-363, 1995

S. Anwar, "Control Algorithm for a Yaw Stability Management System", US Patent Number 6,885,931, April 26, 2005.

Masao Nagai, Motoki Shino, Feng Gao, "Study on Integrated Control of Active Front Steer Angle and Direct Yaw Moment" JSAE Review, pp. 309-315, 23, year 2002.

Johannes Gerhard, Maria-Christina Laiou, Martin Monnigmann, Wolfgan Marquardt, "Robust Yaw Control Design with Active Differential and Active Roll Control Systems". Advances in Automotive Control, IFAC, Salerno, Italy - April 19-23 2004.

S. Frediani, R. Gianoglio and F. Giuliano, "System for the Active Control of a Motor Vehicle Differential", US Patent Number. 6,393,351 B2 May 2002, Applicant Centro Ricerche Fiat.

Y. Ushiroda, K. Sawase and K. Suzuki, "Development of super AYC", New Technologies, n° 15, pp.73-76, 2003.

F. Cheli, M. Giaramita, F. Resta, M. Zanchetta, G. C. Travaglio, "A New Control Strategy for a Semi-Active Differential" 16th IFAC World Congress, Prague, July 3-8, 2005.

M. Canale, L. Fagiano, M. Milanese, P. Borodani, "Robust Vehicle Yaw Control Using Active Differential and Internal Model Control Techniques", Proceeding of the 2006 American Control Conference, Mineapolis, Minesota, USA, June 14-16, 2006

R. Marino, S. Scalzi, F. Cinili, "A Nonlinear Semiactive Rear Differential Control in Rear Wheel Drive Vehicles", Proceeding of the 26th Chinese Control Conference, Zhangjiajie, China, July 26-31, 2007

R. Morselli, R. Zanasi, G. Sandoni, "Mechanical and Active Car Differentials: Detailed and Reduced Dynamic Models" 4TH MATHMOD, Vienna, 2003.

6. APPENDIX

Table 1. Vehicle parameters for the linear model:

m	1300	[kg]	J	1296	[kg m^2]
l_f	0.88	[m]	l_r	1.32	[m]
c_{fy}	9.417e+4	[N/rad]	c_{ry}	7.946e+4	[N/rad]
c_{fx}	1.049e+5	[N]	c_{rx}	7.522e+4	[N]
T_f	1.465	[m]	T_r	1.470	[m]
R_w	0.334	[m]	J_w	0.9	[kg m^2]